PNAS RESEARCH ARTICLE | EARTH, ATMOSPHERIC, AND PLANETARY SCIENCES

Long-term core–mantle interaction explains W-He isotope heterogeneities

Amy L. Ferrick[a,1] and Jun Korenaga[a]

Edited by Peter Kelemen, Lamont-Doherty Earth Observatory, Palisades, NY; received September 16, 2022; accepted December 8, 2022

The isotopic characteristics of ocean island basalts have long been used to infer the nature of their source and the long-term evolution of the Earth's mantle. Anticorrelation between tungsten and helium isotopic signatures is a particularly puzzling feature in those basalts, which no single process appears to explain. Traditionally, the high $^{3}He/^{4}He$ signature has been attributed to an undegassed reservoir in the deep mantle. Additional processes needed to obtain low $^{182}W/^{184}W$ often entail unobserved ancillary geochemical effects. It has been suggested, however, that the core feeds the lower mantle with primordial helium, obviating the need for an undegassed mantle reservoir. Independently, the tungsten-rich core has been suggested to impart the plume source with anomalous tungsten isotope signatures. We advance the idea that isotopic diffusion may simultaneously transport both tungsten and helium across the core–mantle boundary, with the striking implication that diffusion can naturally account for the observed isotopic trend. By modeling the long-term isotopic evolution of mantle domains, we demonstrate that this mechanism can account for more than sufficient isotopic ratios in plume-source material, which, after dynamical transport to the Earth's surface, are consistent with the present-day mantle W-He isotopic heterogeneities. No undegassed mantle reservoir is required, bearing significance on early Earth conditions such as the extent of magma oceans.

isotope heterogeneity | helium | tungsten | core | entrainment

Significance

Ocean island basalts, thought to originate from deep mantle material, exhibit a correlation between tungsten and helium isotopic signatures. The source of this correlation remains elusive: While mantle helium isotope heterogeneities are often attributed to a primitive, undegassed lower mantle reservoir, additional processes must be invoked to further explain the correlation with tungsten isotope signatures. We show that direct interaction between the core and the deep mantle can naturally explain the tungsten and helium isotopic composition of ocean island basalts. This possibility undermines the long-standing view that the processing of the Earth's mantle must be inefficient to preserve primordial signals.

Isotopic heterogeneities in the Earth's mantle provide a window into processes that have shaped the planet during both its infancy and its subsequent evolution. The isotopic characteristics of ocean island basalts (OIBs) are particularly useful tools, as OIBs carry chemical signatures from the deep mantle to the surface. One recently discovered isotopic curiosity of OIBs is the negative correlation between $^{182}W/^{184}W$ and $^{3}He/^{4}He$, two chemically disparate systems (1, 2). OIBs exhibit negative $\mu^{182}W$ as low as −22 (where $\mu^{182}W = 0$ is defined as the ambient mantle and $\mu^{182}W = 10^6 \times \left[(^{182}W/^{184}W)_{sample} - {}^{182}W/^{184}W)_{standard}\right]$) and $^{3}He/^{4}He$ as high as $50R_A$ (where R_A is the atmospheric ratio and the background mantle contains helium with $^{3}He/^{4}He \sim 8R_A$ on average).

Several mechanisms have been invoked to explain the low $^{182}W/^{184}W$ in OIBs relative to the ambient mantle. First, the addition of core components may impart the lower mantle with the highly negative $^{182}W/^{184}W$ signature of the core (2–4), which formed with low Hf/W due to the siderophile nature of tungsten and then developed $\mu^{182}W \sim -220$ when ^{182}Hf decayed to ^{182}W. According to a second hypothesis, a chondritic late veneer may have delivered material with $\mu^{182}W = -200$ to the lower mantle (5). However, direct addition of core components or a chondritic late veneer to the lower mantle would introduce enrichments in highly siderophile elements; OIBs display neither enrichments in highly siderophile elements nor a correlation between $\mu^{182}W$ and tungsten abundance (e.g., ref. 2). In a third scenario, crystal-liquid fractionation while ^{182}Hf was extant would lead to an enriched reservoir with low Hf/W, e.g., Hadean protocrust (6) and a depleted reservoir with high Hf/W (1, 7) due to tungsten's relative incompatibility. However, early crust may not contain sufficiently negative $\mu^{182}W$ to explain OIBs (2) and may not deliver abundant tungsten to the lower mantle, due to extraction of tungsten into subduction fluids (8). Thus, the first two scenarios appear untenable, and the third scenario is questionable. Recently, however, a revision of the core–mantle interaction hypothesis has been proposed that may deliver the isotopic tungsten signature of the core without influencing elemental abundances: diffusive isotopic exchange. Experiments have shown that tungsten self-diffusion in the lower mantle may be efficient (9).

Author affiliations: [a]Department of Earth and Planetary Sciences, Yale University, New Haven, CT 06511

Author contributions: A.L.F. and J.K. designed research; A.L.F. performed research; A.L.F. and J.K. analyzed data; J.K. discussed the results and commented on the paper; and A.L.F. wrote the paper.

The authors declare no competing interest.

This article is a PNAS Direct Submission.

[1]To whom correspondence may be addressed. Email: amy.ferrick@yale.edu.

This article contains supporting information online at http://www.pnas.org/lookup/suppl/doi:10.1073/pnas.2215903120/-/DCSupplemental.

Published January 17, 2023.

The source mechanism of anomalous tungsten in OIBs is still debated, and the situation becomes even more muddied when one tries to explain both negative μ^{182}W and its anticorrelation with ^{3}He/^{4}He.

Elevated ^{3}He/^{4}He in OIBs has traditionally been explained by invoking an undegassed, primitive reservoir in the lower mantle (10–12). Yet, plume-source material exhibits fractionated, nonprimitive isotopic characteristics (13, 14), and thus, the plume-source mantle cannot be primitive, even if it contains primitive ^{3}He. Still, a relatively undegassed mantle reservoir (if not fully pristine) might preserve primitive ^{3}He, and this idea is still common. The presence of relatively undegassed mantle material requires that mantle mixing, which promotes degassing, must be inefficient. Although primitive ^{3}He may be preserved during subsolidus mantle convection (15, 16), a relatively undegassed reservoir must have also survived the vigorously convecting magma ocean stage of the Earth's mantle. Since magma oceans likely degassed fairly efficiently, a whole-mantle magma ocean must be avoided in order for significant primitive mantle ^{3}He to survive.

Indeed, a molten mantle likely loses its helium quickly. Turnover in magma oceans is rapid, with convective velocities up to 10 m/s, so that the entire magma ocean is processed quickly relative to its lifetime (17). While water degassing may be inefficient due to its high solubility, helium degassing is likely to be similar to that of carbon dioxide, which has a low magma solubility (18). Thus, maintaining a relatively undegassed reservoir during planetary accretion requires special conditions to keep some fraction of impactors unmolten as well as to avoid a whole-mantle magma ocean.

The undegassed reservoir hypothesis must further be paired with an additional mechanism to explain the correlation with tungsten isotopes as high ^{182}W/^{184}W does not naturally arise within undegassed material. This is true even for more exotic candidates for an undegassed mantle reservoir (as opposed to a silicate reservoir), such as suspended primordial metallic melt, which would not introduce anomalous tungsten isotopes (19). Several multistage models have been proposed to accommodate observed isotopic signatures of both helium and tungsten. For example, Hadean protocrust with negative μ^{182}W may have been recycled into an undegassed mantle reservoir (6). However, recycled crust would also mix with background (degassed) mantle material, leading to basalts with negative μ^{182}W and ambient ^{3}He/^{4}He, which is not observed. Another model invokes isotopic equilibration between the core and a molten silicate layer to impart negative μ^{182}W to an undegassed mantle reservoir (2). This material is prescribed an undegassed nature, but if the molten silicate layer is the residue of a magma ocean, as proposed, it will likely be degassed. The task of explaining the negative μ^{182}W-^{3}He/^{4}He correlation in OIBs is evidently fraught with complexity.

The shortcomings of the partially undegassed mantle hypothesis have prompted an alternative scenario. Although often prescribed to explain the presence of ^{3}He in mantle-derived rocks, an undegassed mantle reservoir requires fortuitous circumstances: Primordial helium must survive several processes throughout the Earth's history that have subjected the mantle to degassing, including melt-inducing giant impacts (20), mantle overturns during magma ocean solidification (21), and billions of years of mantle convection (22). Once in the atmosphere, helium is not recycled back into the mantle. In light of this issue, some have proposed not the lower mantle itself but the Earth's core as a reservoir of primordial helium that feeds the lower mantle (23–25). Helium partitioning experiments indicate that the core may house large amounts of primordial helium (24), which may then migrate to the deep mantle via diffusive equilibration (25).

In addition to high ^{3}He/^{4}He, OIBs also exhibit solar-like ^{3}He/^{22}Ne (26). This suggests a common source of primordial helium and neon, and some have questioned the ability of these two elements to remain unfractionated during core formation and subsequent core–mantle interaction, due to a large apparent disparity between neon and helium partitioning (27). However, these partitioning experiments are not valid for the formation of the Earth's core, which takes place via accretion of planetesimal cores. Helium and neon remain unfractionated at conditions of planetesimal core formation (28). Only small amounts of these cores are needed to dominate the ^{3}He/^{22}Ne signature of the Earth's core (28), and metal–silicate mixing models indicate that cores of giant impactors can indeed incorporate directly into the Earth's core before equilibrating with the mantle (29). Helium and neon may also remain unfractionated during subsequent transfer of these elements to the plume source, as experiments have supported the idea that all noble gases partition similarly (30, 31). Recently, this idea has been questioned based on noble gas partitioning between liquid metal and silicate melt (27), but it is the partitioning between liquid metal and solid silicate that is relevant for diffusive transport across the core–mantle boundary (CMB). Given that helium and neon are expected to have similar solubilities in bridgmanite (32), their partitioning between liquid metal and bridgmanite is likely to be similar (33). Further, metal–silicate noble gas partitioning is several orders of magnitude higher at conditions of planetesimal core formation than at conditions of the present-day core–mantle boundary (28). Thus, not only are noble gases likely to be amply supplied to the Earth's core upon incorporation of planetesimal cores, a large disequilibrium is achieved at the CMB, which ultimately drives core–mantle diffusion.

Remarkably, therefore, the Earth's core may act as a reservoir of both tungsten and helium isotopes, which are fed to the lower mantle via isotopic diffusion, thereby simultaneously accounting for the tungsten and helium isotopic signatures of the plume-source mantle. Diffusive gradients of core-like tungsten and helium isotopes may naturally explain the observed μ^{182}W–^{3}He/^{4}He correlation in OIBs. To quantitatively assess this possibility, we model the long-term isotopic evolution of the ambient mantle and plume-source mantle, assuming the operation of diffusive isotopic exchange with the core. Combined with a geodynamical calculation of the degree of entrainment of plume-source material, our model reproduces the tungsten and helium characteristics of OIBs, with no need for invoking additional mechanisms. A core origin for undegassed helium holds very different implications for processes in the Earth's early mantle than a mantle origin, as an undegassed mantle reservoir suggests incomplete mantle melting and prolonged convective isolation (11).

^{182}W/^{184}W Evolution of the Plume-Source Mantle

The hotspots that generate OIBs originate from deep-rooted mantle plumes, the sources of which are often associated with large low shear velocity provinces (LLSVPs), seismically anomalous regions in the lower mantle (34). Material near the base of LLSVPs is expected to be gravitationally stable and thus long-lived, allowing for the core's ^{182}W/^{184}W signature

to accumulate over potentially billions of years via diffusive exchange (Fig. 1*A*). At the same time, CMB regions not occupied by dense, long-lived material accumulate the core tungsten signature over shorter timescales, followed by mixing into the background mantle (Fig. 1*A*), reducing its μ^{182}W over time to the present-day value of 0. Assuming core–mantle equilibrium with respect to tungsten concentrations, diffusion occurs via self-diffusion in which tungsten atoms exchange with one another, thereby reducing the μ^{182}W gradient across the CMB. Tungsten is much more abundant in the metallic core, such that the core can continuously supply the lower mantle with tungsten characterized by $\mu^{182}\mathrm{W} = -220$. Because there are no other major tungsten fluxes (it is likely that most of continental growth, and thus extraction of tungsten from the mantle, occurred before 4 Gya (35)), the evolution of ^{182}W/^{184}W in a long-lived plume-source reservoir can be characterized simply by a diffusion length, $L = \sqrt{\kappa_W \tau}$, where κ_W is tungsten diffusivity in the lower mantle and τ is the lifetime of the material at the CMB. Diffusivity depends on lower mantle grain size, which may differ for the background mantle and a long-lived reservoir (36). Using $\tau = 4$ Ga for the dense plume-source reservoir, along with appropriate κ_W (*Methods*), yields $L \sim 5$ to 10 km (*SI Appendix*, Fig. S1); this is the height above the CMB that the full core signature of $\mu^{182}\mathrm{W} = -220$ penetrates over the timescale τ. Although the height of seismically observed dense regions above the CMB is an order of magnitude larger than this diffusion length (37), mantle plume locations correlate with the margins of LLSVPs (38) where they are thinnest. According to a diffusive vertical profile, it is these thin margins that would carry the most core-like isotopic signature. Thus, $\mu^{182}\mathrm{W} = -220$ can be considered an upper bound of the plume-source tungsten isotopic signature.

The ancient Archean mantle was characterized by ^{182}W/^{184}W 10 to 15 ppm higher than the modern upper mantle (5). It has been proposed that late accretion of bulk chondritic material and its subsequent mixing with the mantle may explain the decrease in μ^{182}W over time (5), although an analysis of tungsten and neodymium isotopes in Archean rocks favors a deep-seated origin (39). Our simple diffusion model allows us to quantify the effect of core–mantle interaction on the long-term evolution of mantle μ^{182}W, as isotopic exchange will operate not only between the core and the plume source but also between the core and the background mantle, as noted above. Assuming reasonable lower mantle grain sizes, core–mantle diffusion can lower the background mantle μ^{182}W by 5 to 7 ppm and possibly more in the case of small grain size (*Materials and Methods*). Any further decrease in terrestrial μ^{182}W can plausibly be explained by a small addition of late accreted material.

^{3}He/^{4}He Evolution of Mantle Domains

Unlike tungsten, which is subject to self-diffusion across the CMB, helium is subject to a nonzero net flux across the CMB, due to the large disequilibrium in concentration induced by mantle degassing. A simple diffusion length is insufficient to characterize helium evolution, given additional sources and sinks of ^{3}He and ^{4}He. We model ^{3}He and ^{4}He in the core, background mantle, and a long-lived plume-source reservoir forward in time starting from a fully degassed mantle at 4 Gya. We then evaluate the success of the core–mantle interaction model in predicting present-day observations of mid-ocean ridge basalts (MORB) and OIBs.

The change in background mantle ^{3}He and ^{4}He concentrations over time is balanced by the fluxes into and out of the reservoir (Fig. 1*B*). Diffusion across the CMB and from the plume source to the background mantle contributes ^{3}He and ^{4}He, surface degassing removes ^{3}He and ^{4}He, and radiogenic isotopes of U and Th produce ^{4}He. Surface outgassing is controlled by the concentration of an isotope as well as the mantle processing rate, the latter of which we assume is constant over 4 Ga (40). The flux of ^{3}He and ^{4}He from the core to the mantle is primarily controlled by the disequilibrium of ^{3}He and ^{4}He concentrations at the CMB (25), which is large due to extensive mantle degassing expected during the early Earth. Analogously, the diffusive flux between the background mantle and the plume-source reservoir is controlled by the concentration gradients of ^{3}He and ^{4}He between the two reservoirs (which tends to favor transfer from the plume source to the background mantle). The plume-source reservoir is subject to a slightly different set of fluxes than the background mantle (Fig. 1*B*). Instead of surface

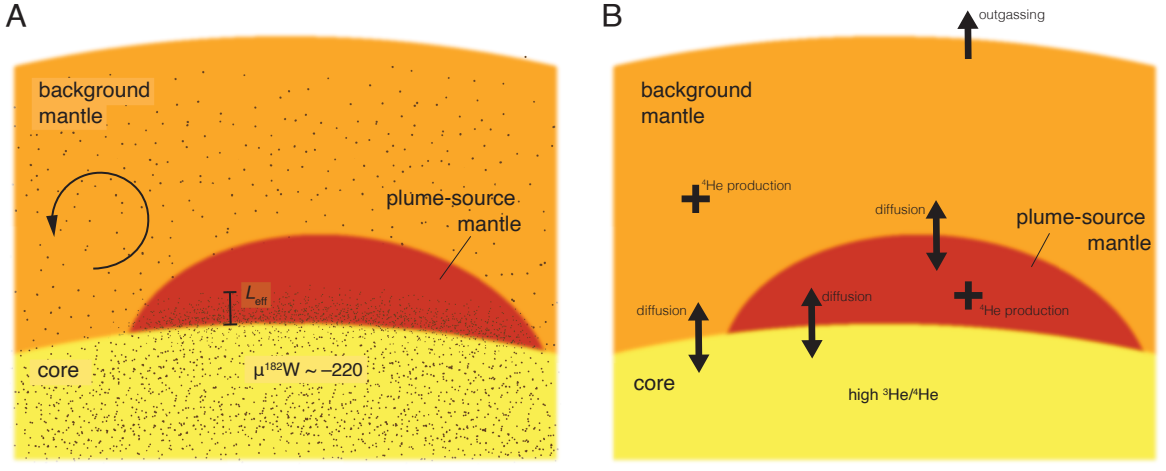

Fig. 1. Conceptual model for (*A*) tungsten and (*B*) helium evolution. (*A*) The core μ^{182}W signature diffuses into mobile background mantle material with a CMB lifetime of 100 Ma, after which mixing with the overlying mantle occurs. Simultaneously, diffusion occurs between the core and a plume-source mantle reservoir, where material is static and the core μ^{182}W signature builds up over ~4 Ga. (*B*) The background mantle concentration in ^{3}He and ^{4}He is governed primarily by diffusion across the CMB (driven by the CMB concentration gradient), outgassing at the surface (proportional to a time-invariant mantle processing rate *r*), and radiogenic production of ^{4}He. A plume-source mantle reservoir above the CMB is not subject to outgassing, but it is subject to diffusion across the boundary with the overlying background mantle.

outgassing, ^{3}He and ^{4}He are lost via the diffusive flux between the background mantle and the plume source.

The helium concentration in the Earth's core is largely unconstrained, so we randomly sample for initial core ^{3}He concentration. We calculate core ^{4}He concentration using the core's ^{3}He/^{4}He, which may be as large as 330 R_A if accretion occurred after solar deuterium burning (41). Additional parameters we randomly sample for include helium diffusivity, metal–silicate partition coefficient, bulk mantle radiogenic heat production, and enrichment of the plume-source reservoir in heat-producing elements (*SI Appendix*, Table S2). Depending on how the plume-source reservoir formed, it may be enriched in incompatible elements with respect to the background mantle.

We run 5×10^5 models, each time randomly sampling for the five parameters listed above. In order for a model to be successful, it must reproduce the observed present-day helium characteristics of the background mantle (i.e., MORB) and the plume source (i.e., OIBs). At present-day, ^{3}He/^{4}He in MORB is 8 R_A, and we allow for ± 2 R_A of uncertainty. Helium concentrations are less straightforward to measure than isotopic ratios. A reasonable lower bound for ^{3}He concentration in MORB-source mantle is 8.33×10^{-16} mol/g (or 5.19×10^8 at/g) (25). We take twice this concentration as the upper limit. Finally, OIBs exhibit ^{3}He/^{4}He up to 50 R_A. In our modeling approach, we track average helium concentrations across a given reservoir; in reality, the long-lived plume-source reservoir will exhibit a diffusive concentration profile, with higher concentrations near the core–mantle boundary. Thus, even if the average ^{3}He/^{4}He is less than 50 R_A for a given model, OIBs may still contain high ^{3}He/^{4}He depending on the depth at which plume-source material is entrained. To account for this, we consider all models for which average ^{3}He/^{4}He > 10 R_A successful. Approximately 2% of models satisfy all three criteria, for a total of $\sim 10^4$ successful models.

In successful cases, ^{3}He concentration increases over time in both the background mantle and the plume source (Fig. 2) due to the core–mantle boundary flux. The plume-source reservoir is more concentrated in ^{3}He because of its small size and long lifetime above the CMB. Initially, ^{3}He/^{4}He is relatively high in both mantle reservoirs (Fig. 2), due to the instantaneous flux of high–^{3}He/^{4}He helium from the core at 4 Gya. Over time, ^{3}He/^{4}He decreases over time in both mantle reservoirs because ^{4}He increases in greater proportion than ^{3}He, due to the radiogenic flux. Core helium concentration decreases over time as CMB diffusion continues; in all cases, this decrease is extremely minor, such that the core concentration of ^{3}He and ^{4}He can be considered constant.

Present-day mantle helium characteristics are primarily a function of core helium concentration (Fig. 3). As initial core helium increases, so do present-day background mantle ^{3}He, background mantle ^{3}He/^{4}He, and plume-source reservoir ^{3}He/^{4}He. Even so, successful models are produced across the entire range of core helium concentrations that we test (Fig. 3).

Thus, core–mantle helium diffusion can supply a long-lived plume-source reservoir with average ^{3}He/^{4}He in excess of 50 R_A at present day (Figs. 2 and 3). Our model allows for complete mantle degassing in the time period prior to 4 Ga. We do not model this time period as it is unnecessary for investigating core–mantle interaction and involves several poorly constrained early Earth processes.

Entrainment Dynamics of Core-Altered Material

Prediction of $\mu^{182}\mathrm{W} \leq -22$ and ^{3}He/^{4}He $\geq 50R_A$ in the plume-source reservoir does not guarantee sufficiently low μ^{182}W or high ^{3}He/^{4}He in erupted basalts. A long-lived reservoir, due to its dense and dynamically stable nature, does not rise on its own. Rather, it is thought that hot mantle plumes with background composition originate near the margins of compositionally distinct domains (38, 42) and may entrain neighboring dense material (43, 44). The degree of entrainment is primarily controlled by the ratio of negative chemical buoyancy in the dense material, $\Delta\rho_{Ch}$, to positive thermal buoyancy in the hot upwelling material, $\Delta\rho_T$ (43, 44). For upwellings with uniform velocity and cylindrical geometry, the volume ratio of entrained dense material to total upwelling material is maximally $(\Delta\rho_T/\Delta\rho_{Ch})^2$ (43). Using estimates of compositional density anomalies in LLSVPs (45, 46), this simple dynamical calculation implies that 11% of upwellings are composed of dense entrained material (*Methods*). It should be noted, however, that the density structure of LLSVPs is still poorly constrained (47).

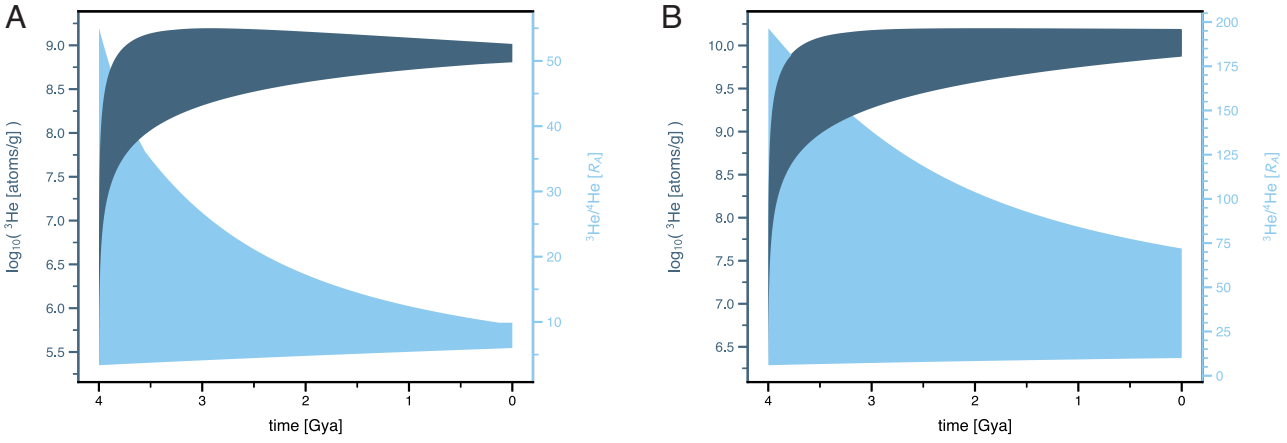

Fig. 2. Helium evolution of all successful cases. (*A*) Evolution of ^{3}He abundance and ^{3}He/^{4}He in the background mantle. (*B*) Evolution of ^{3}He abundance and ^{3}He/^{4}He in the plume-source mantle.

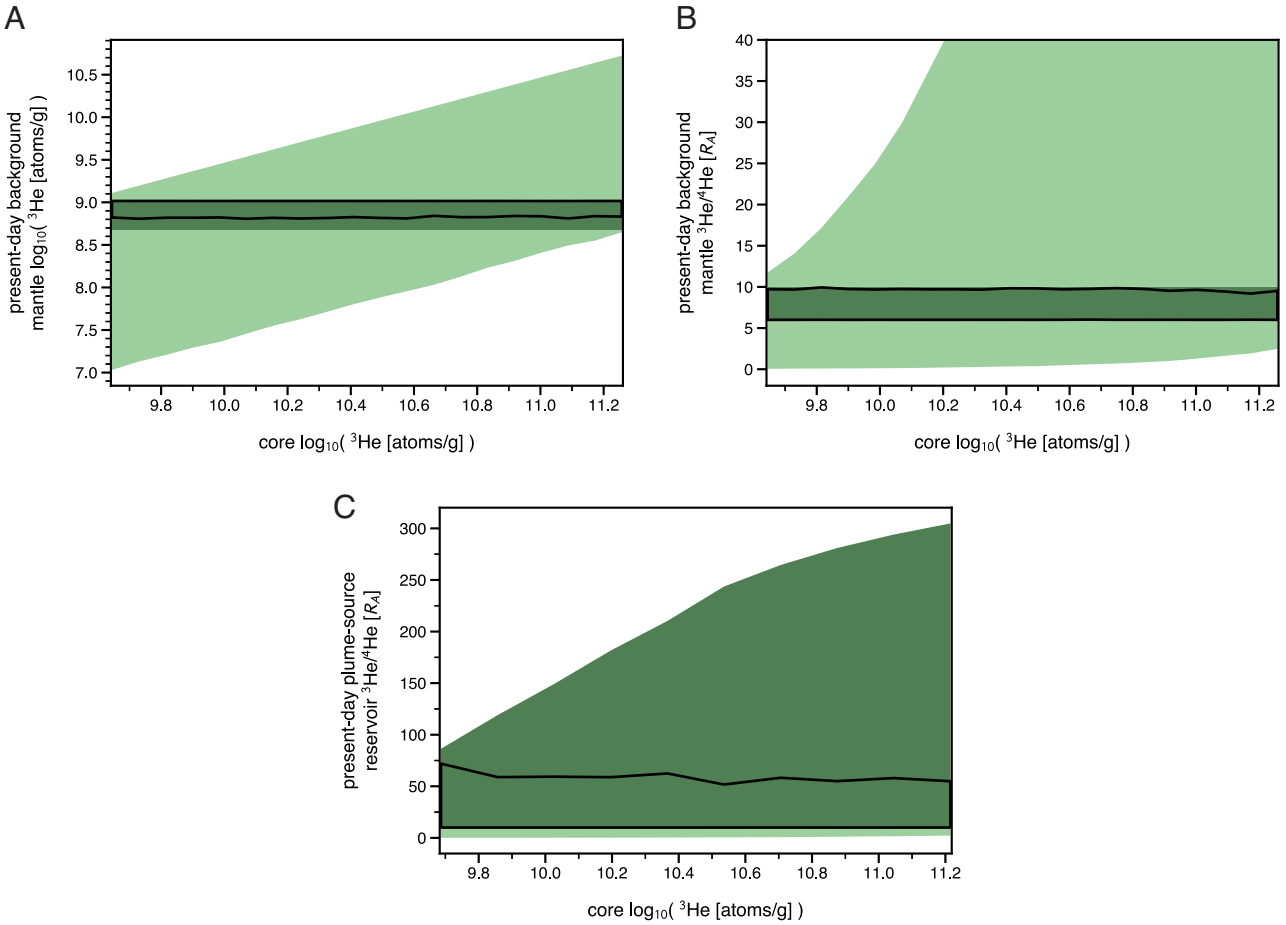

Fig. 3. Helium evolution results as a function of core helium concentration. (*A*) Present-day abundance of ^{3}He in the background mantle, (*B*) present-day ^{3}He/^{4}He in the background mantle, and (*C*) present-day ^{3}He/^{4}He in the plume-source reservoir. Dark green indicates cases that satisfy the success criterion relevant to the displayed parameter (i.e., 5.19×10^8 at/g $< C_{3,M} < 1.04 \times 10^9$ at/g, $6\ R_A < C_{3,M}/C_{4,M} < 10\ R_A$, and $C_{3,plume}/C_{4,plume} > 10\ R_A$ for panels *A*, *B*, and *C*, respectively). Black lines contain the successful cases (i.e., those that satisfy all three success criteria).

Assuming a uniform tungsten concentration in the mantle, upwellings composed of 11% dense, core-altered material (with $\mu^{182}W = -220$) and 88% background mantle (with $\mu^{182}W = 0$) will have a bulk composition of $\mu^{182}W = -22$. This lower bound is in good agreement with the most negative $\mu^{182}W$ observed in OIBs (2).

A given helium evolution model describes the average ^{3}He and ^{4}He concentration in the plume-source reservoir, which is not equivalent to the ^{3}He and ^{4}He concentration near the base (i.e., thin margins) of the reservoir, where material is likely to be entrained. For each He evolution model, we calculate a diffusive vertical concentration gradient for ^{3}He and ^{4}He that we use to determine ^{3}He/^{4}He near the base of the reservoir (*SI Appendix*, Fig. S2*A* and *Methods*). When calculating the bulk composition of upwellings, we account for differences in ^{3}He and ^{4}He concentration with respect to the background mantle.

Assuming the average background mantle He content, upwellings with ^{3}He/^{4}He $\geq 50R_A$ are achieved for all of the models satisfying the three success criteria. When we consider that 1) plume-source material may mix with background mantle material that deviates from the average background mantle composition (e.g., ^{3}He/^{4}He > 8 and $\mu^{182}W > 0$); 2) concentration-driven diffusion may not be uniform across all plume-source material, whose residence time at the CMB can vary; and 3) material may be entrained at different depths along the diffusive isotopic profiles in the plume-source reservoir; the full range of OIB ^{182}W–^{3}He observations can be explained (Fig. 4).

Implications for Mantle Evolution

An undegassed mantle reservoir, traditionally invoked to explain high ^{3}He/^{4}He in OIBs, may require incomplete mantle melting in the early Earth, as magma oceans entail extensive degassing. However, we have shown that core-derived primordial helium alone can explain OIB isotopic signatures, thus placing no restriction on the degree of early degassing and thus the degree of early mantle melting. Under our hypothesis, a whole-mantle magma ocean is allowed and perhaps even necessary. Specifically, a basal magma ocean—the result of a whole-mantle magma ocean that begins crystallizing at an intermediate depth—is thought to naturally leave behind dense thermochemical piles (48, 49). Dense, gravitationally stable material is required for core isotopic signatures to accumulate in the plume source for sufficiently long periods of time, so a basal magma ocean may be favorable for achieving OIB-like tungsten and helium signatures. It should be noted that alternative scenarios may also generate thermochemical piles, such as the gravitational segregation of recycled oceanic crust in the deep mantle (50–52). This scenario

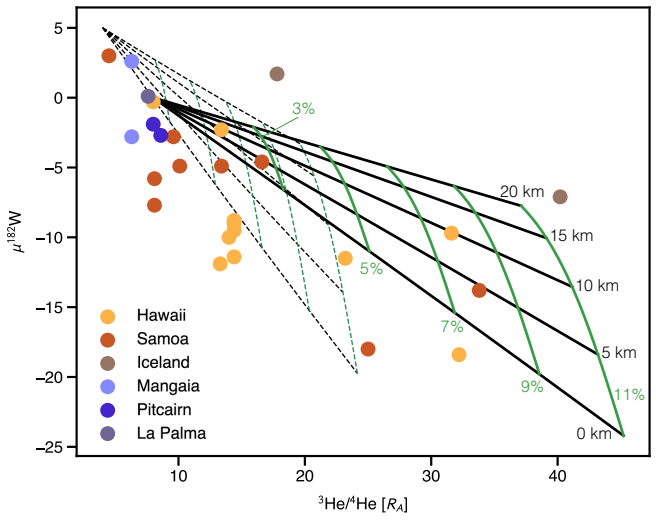

Fig. 4. μ^{182}W–^{3}He/^{4}He of OIBs and model prediction. Colored symbols show measurements of OIBs (1). For a representative successful helium evolution model, we calculate the diffusive vertical profiles of μ^{182}W, ^{3}He concentration, and ^{4}He concentration. Since tungsten diffusivity is lower than helium diffusivity, entrainment at different depths leads to variation in the μ^{182}W-^{3}He/^{4}He trend. Black and green curves enclose the range of expected compositions, assuming two-component mixing between plume-source material and average background mantle material (solid) and background mantle material with high μ^{182}W and low ^{3}He/^{4}He (dashed). To obtain this low ^{3}He/^{4}He composition, we increase the concentration of ^{4}He from the average background mantle value. Black curves indicate the height below which the plume source is sampled (we take the average composition of plume source material between the CMB and this height), and green curves indicate degree of entrainment (fraction of upwelling material that is composed of plume-source material), up to the estimated maximum degree of entrainment.

has the benefit of explaining additional chemical features of OIBs (50).

The presence of primordial ^{3}He in the Earth's mantle has further been used as evidence of convective isolation of a lower mantle reservoir throughout the Earth's history (11), although this may not be necessary under certain conditions of slab recycling and mixing (16). By invoking the core as the source of undegassed helium, our model relaxes these constraints on the history of mantle mixing. We require a lower mantle reservoir to be dynamically stable for a few billion years, as opposed to the whole of the Earth's history. LLSVPs offer an observational basis for the presence of such dynamically stable material. Further, our model is consistent with the recently revitalized concept of a permanently buried early enriched reservoir to explain mantle isotopic characteristics (14).

The diffusional core–mantle interaction modeled here is inevitable if tungsten and helium are sufficiently mobile at the CMB. Large grain sizes can hinder efficient grain boundary diffusion, and while it is thought that chemically dense deep mantle material bears large grain sizes due to inefficient mixing (53), tungsten may diffuse tens of kilometers over billion-year timescales even with these large grain sizes (9). Diffusion of helium into the lower mantle relies on sufficient core helium abundance (Fig. 3). Based on partitioning experiments, significant helium may have been incorporated into the core upon its formation (24, 28). Subsequent extensive mantle degassing is likely, thereby establishing a disequilibrium that drives helium transfer across the CMB. Therefore, the presence of core-like signatures of both tungsten and helium in the deep mantle is readily explained.

Materials and Methods

Tungsten Diffusion. The diffusive propagation of the core ^{182}W/^{184}W signature into the lower mantle is described by a characteristic length scale:

$$L = \sqrt{\kappa_W \tau}, \quad [1]$$

where κ_W is tungsten diffusivity and τ is material residence time at the CMB. Tungsten diffusivity is an effective value from the combination of lattice diffusion and grain boundary diffusion:

$$\kappa_W = \kappa_l + 3\delta\kappa_{gb}/d, \quad [2]$$

where κ_l is lattice diffusivity, κ_{gb} is grain boundary diffusivity, δ is grain boundary width, and d is grain size. We assume that lattice diffusion is negligible (9) and calculate the product $\delta\kappa_{gb}$ from an Arrhenius relationship:

$$\delta\kappa_{gb} = \delta\kappa_{gb,0}\exp\left[-\frac{E+PV}{RT}\right], \quad [3]$$

where $\delta\kappa_{gb,0}$ is $\delta\kappa_{gb}$ at standard state, E is activation energy, P is pressure, V is molar volume, R is the universal gas constant, and T is temperature. We calculate κ_{gb} using the measurements of ref. 9 and reasonable lower mantle conditions (*SI Appendix*, Table S1). It should be noted that as the plume-source mantle accumulates the core μ^{182}W signature, the background mantle also exchanges tungsten isotopes with the core, lowering its μ^{182}W to the present-day value of 0. Assuming that background mantle material above the CMB recycles every 100 Ma, and that the background mantle and plume-source mantle occupy 80% and 20% of the CMB surface area, respectively (34), we calculate an effective diffusion length of ~3 km and a decrease in the background mantle of about five units μ^{182}W over 4 Ga. Thus, both the background mantle and plume-source reservoir (which formed from ambient mantle) were characterized by μ^{182}W = 5 at 4 Gya.

Helium Flux Modeling. The evolution of ^{3}He and ^{4}He in the background mantle is governed by the following flux balances:

$$M_M\frac{dC_{3,M}}{dt} = F_{3,M}^{\mathrm{CMB}} + F_3^{MM} - F_{3,M}^S, \quad [4]$$

$$M_M\frac{dC_{4,M}}{dt} = F_{4,M}^{\mathrm{CMB}} + F_4^{MM} - F_{4,M}^S + F_{4,M}^R, \quad [5]$$

where M_M is mantle mass, $C_{i,M}$ is the concentration of a given isotope, $F_{i,M}^{CMB}$ is diffusive flux of an isotope at the CMB, F_i^{MM} is the diffusive flux of an isotope at the mid-mantle interface between the background mantle and the plume-source reservoir (where a flux into the background mantle is taken as positive), $F_{i,M}^S$ is the surface flux of an isotope due to volcanic outgassing, and $F_{4,M}^R$ is radiogenic production of ^{4}He. The surface flux of an isotope i is proportional to the concentration $C_{i,M}$ of the isotope and the mantle processing rate r, the latter of which we assume is constant over the last 4 Ga (40):

$$F_i^S = rC_{i,M}. \quad [6]$$

Radiogenic production of ^{4}He occurs via decay of ^{238}U, ^{235}U, and ^{232}Th:

$$F_{4,M}^R = -8\frac{\mathrm{d}N_{238,M}}{\mathrm{d}t} - 7\frac{\mathrm{d}N_{235,M}}{\mathrm{d}t} - 6\frac{\mathrm{d}N_{232,M}}{\mathrm{d}t}, \quad [7]$$

where $N_{j,M}$ is the number of atoms of a given isotope present in the background mantle, which decays exponentially:

$$N_j(t) = N_{j,0}\exp\left(t'\lambda_j\right), \quad [8]$$

where $N_{j,0}$ is the present-day number of atoms, t' is time before the present, and λ_j is an isotope's decay constant. The $N_{j,0}$ are calculated from the present-day radiogenic heat production in the background mantle, $H_{M,0}$, and the heat

generation rate of the heat-producing elements (see, e.g., ref. 54). The relative contributions of the background mantle and plume-source reservoir to the bulk mantle heat production, $H_{tot,0}$, are determined by an enrichment factor, e, describing the enrichment of heat-producing elements in plume-source material with respect to background mantle material:

$$H_{M,0} = H_{tot,0}\left(1 - \frac{M_P}{M_M}e\right), \quad [9]$$

$$H_{P,0} = H_{tot,0} - H_{M,0}, \quad [10]$$

where M_P is the mass of the plume-source reservoir. With an enrichment factor of 1, the background mantle plume-source mantle contains equal concentrations of heat-producing elements. The diffusive flux is driven by the deviation from core–mantle equilibrium at the CMB, which is mediated by helium partitioning:

$$F_{i,M}^{CMB} = \rho_M\left(\frac{C_{i,C}}{D} - C_{i,M}\right)(1-f)A_{\mathrm{CMB}}v_M, \quad [11]$$

where ρ_M is mantle density, $C_{i,C}$ is the core concentration of an isotope, D is the helium metal/silicate partition coefficient, f is the fraction of CMB surface area occupied by plume-source material, and A_{CMB} is CMB surface area. The diffusion velocity, $v_M = \sqrt{2\kappa_{\mathrm{He}}\tau_M/\pi}$, depends on helium diffusivity, κ_{He}, and material residence time at the CMB, τ_M, and is constant over time. The mid-mantle diffusive flux is governed analogously to Eq. **11**:

$$F_{i,M}^{MM} = \rho_M\left(C_{i,P} - C_{i,M}\right)(1-f)A_{MM}v_M, \quad [12]$$

where $C_{i,P}$ is the concentration of an isotope in the plume-source reservoir, and A_{MM} is the surface area of the mid-mantle interface (i.e., the entire spherical shell), which we calculate assuming that the plume-source reservoir is 150-km thick.

^{3}He and ^{4}He in the plume-source reservoir are governed by a similar set of fluxes:

$$M_P\frac{dC_{3,P}}{dt} = F_{3,P}^{\mathrm{CMB}} - F_3^{MM}, \quad [13]$$

$$M_P\frac{dC_{4,P}}{dt} = F_{4,P}^{\mathrm{CMB}} - F_4^{MM} + F_{4,P}^{R}. \quad [14]$$

Here, the subscript "P" denotes the plume-source reservoir. Diffusion at the CMB is controlled by disequilibrium of isotope concentration between the core and the plume-source reservoir:

$$F_{i,P}^{\mathrm{CMB}} = \rho_M\left(\frac{C_{i,C}}{D} - C_{i,P}\right)fA_{\mathrm{CMB}}v_P, \quad [15]$$

where $v_P = \sqrt{2\kappa_{\mathrm{He}}\tau_P/\pi}$.

Finally, ^{3}He and ^{4}He in the core are simply governed by the following:

$$M_C\frac{dC_{3,C}}{dt} = -F_{3,M}^{\mathrm{CMB}} - F_{3,P}^{\mathrm{CMB}}, \quad [16]$$

$$M_C\frac{dC_{4,C}}{dt} = -F_{4,M}^{\mathrm{CMB}} - F_{4,P}^{\mathrm{CMB}}. \quad [17]$$

Here, the subscript "C" denotes the core, and it is implicit that there is no radiogenic source of ^{4}He in the core. Parameters used in the helium evolution modeling are listed in *SI Appendix*, Table S2.

Entrainment Calculation. The degree of entrainment of dense material neighboring hot upwelling background mantle depends on the ratio of the thermal density anomaly in the hot material, $\Delta\rho_T$ to the chemical density anomaly in the dense material, $\Delta\rho_{Ch}$:

$$R_{\max} = \left(\Delta\rho_T/\Delta\rho_{Ch}\right)^2, \quad [18]$$

where $R_{\max}$ is the upper bound of the ratio of entrained (i.e., dense) material to total material (43). This relationship is valid for three-dimensional (3D) (i.e., cylindrical) plumes, as opposed to two-dimensional (2D) (i.e., sheet-like) plumes, which is appropriate for deep-rooted plumes in the Earth's mantle. The thermal density anomaly depends on a temperature anomaly as $\Delta\rho_T = \rho_M\Delta T\alpha$, where α is thermal expansivity. We estimate the chemical density anomaly from density measurements of LLSVPs (45, 46), taking into account that a positive chemical density anomaly will be larger than the measured density anomaly in the presence of a negative thermal density anomaly. Parameters used in the entrainment calculation are listed in *SI Appendix*, Table S3.

We calculate a maximum degree of entrainment of $R_{\max} = 0.11$. Using this $R_{\max}$, we calculate isotopic composition across the range of mixing proportions up to $R_{\max}$. The end-member plume-source μ^{182}W is −220 (Main Text). Our He flux modeling tracks the bulk ^{3}He and ^{4}He in a reservoir, so the end-member plume-source ^{3}He/^{4}He for a given He evolution model must be determined from diffusive profiles constructed from the bulk ^{3}He and ^{4}He in the plume-source reservoir. The vertical concentration profile above the CMB can be approximated as instantaneous diffusion of a half-space (*SI Appendix*, Fig. S2*A*):

$$C_i(y,t) = (C_{i,\infty} - C_{i,0})\mathrm{erfc}\left[\frac{y}{2\kappa_{\mathrm{He}}t}\right], \quad [19]$$

where y is the vertical distance above the CMB, t is time elapsed, $C_{i,\infty}$ is an isotope's concentration at infinite distance from the CMB, $C_{i,0}$ is an isotope's concentration at the CMB (held fixed), and erfc is the complementary error function. The CMB boundary condition, $C_{i,0}$, is determined from the CMB equilibrium value assuming that the core can continually supply helium: $C_{i,0} = C_{i,C}/D$. This diffusive profile is justified by the consistency of its vertical average after 4 Ga with a reservoir subject to 4 Ga of the diffusive flux used in the model (Eq. **15**), assuming the same boundary and diffusive conditions (*SI Appendix*, Fig. S2*B*). For each helium evolution model, we solve for the $C_{3,\infty}$ and $C_{4,\infty}$ that produce the same present-day average plume-source C_3 and C_4 predicted by the model. We assume the D, κ_{He}, and core helium concentration used in the given model, an elapsed time of 4 Ga, and a plume-source reservoir thickness of 150 km. Once the diffusive profile is fully determined, the end-member plume-source C_3 and C_4 (i.e., those used for mixing with background mantle material) are taken as the average values within the lowermost 50 km of the reservoir. When calculating the bulk upwelling ^{3}He and ^{4}He concentration for a given degree of entrainment, we take into account differences in helium concentration between background mantle material and plume-source material.

Data, Materials, and Software Availability. All study data are included in the article and/or *SI Appendix*.

ACKNOWLEDGMENTS. We thank Al Hofmann and one anonymous reviewer for insightful and constructive reviews. This work was supported in part by NSF EAR–2102777.

1. A. Mundl *et al.*, Tungsten-182 heterogeneity in modern ocean island basalts. *Science* **356**, 66–69 (2017).
2. A. Mundl-Petermeier *et al.*, Anomalous ^{182}W in high ^{3}He/^{4}He ocean island basalts: Fingerprints of Earth's core? *Geochim. Cosmochim. Acta* **271**, 194–211 (2020).
3. L. A. Hayden, E. B. Watson, A diffusion mechanism for core-mantle interaction. *Nature* **450**, 709–711 (2007).
4. H. Rizo *et al.*, ^{182}W evidence for core-mantle interaction in the source of mantle plumes. *Geochem. Perspect. Lett.* **11**, 6–11 (2019).
5. M. Willbold, T. Elliott, S. Moorbath, The tungsten isotopic composition of the Earth's mantle before the terminal bombardment. *Nature* **477**, 195–198 (2011).
6. J. Tusch *et al.*, Long-term preservation of Hadean protocrust in Earth's mantle. *Proc. Natl. Acad. Sci. U.S.A.* **119**, e2120241119 (2022).
7. S. M. Brown, L. T. Elkins-Tanton, R. J. Walker, Effects of magma ocean crystallization and overturn on the development of ^{142}Nd and ^{182}W isotopic heterogeneities in the primordial mantle. *Earth Planet. Sci. Lett.* **408**, 319–330 (2014).
8. S. König, C. Münker, S. Schuth, D. Garbe-Schönberg, Mobility of tungsten in subduction zones. *Earth Planet. Sci. Lett.* **274**, 82–92 (2008).
9. T. Yoshino, Y. Makino, T. Suzuki, T. Hirata, Grain boundary diffusion of W in lower mantle phase with implications for isotopic heterogeneity in oceanic island basalts by core-mantle interactions. *Earth Planet. Sci. Lett.* **530**, 115887 (2020).

10. J. Lupton, H. Craig, Excess ^{3}He in oceanic basalts: Evidence for terrestrial primordial helium. *Earth Planet. Sci. Lett.* **26**, 133–139 (1975).
11. C. J. Allègre, T. Staudacher, P. Sarda, Rare gas systematics: Formation of the atmosphere, evolution and structure of the Earth's mantle. *Earth Planet. Sci. Lett.* **81**, 127–150 (1987).
12. K. Farley, J. Natland, H. Craig, Binary mixing of enriched and undegassed (primitive?) mantle components (He, Sr, Nd, Pb) in Samoan lavas. *Earth Planet. Sci. Lett.* **111**, 183–199 (1992).
13. A. Zindler, S. Hart, Chemical geodynamics. *Annu. Rev. Earth Planet. Sci.* **14**, 493–571 (1986).
14. A. W. Hofmann, C. Class, S. L. Goldstein, Size and composition of the MORB+ OIB mantle reservoir. *Geochem. Geophys. Geosyst.* **23**, e2022GC010339 (2022).
15. C. Class, S. L. Goldstein, Evolution of helium isotopes in the Earth's mantle. *Nature* **436**, 1107–1112 (2005).
16. H. M. Gonnermann, S. Mukhopadhyay, Preserving noble gases in a convecting mantle. *Nature* **459**, 560–563 (2009).
17. V. Solomatov, "Fluid dynamics of a terrestrial magma ocean" in *Origin of the Earth and Moon*, R. M. Canup, K. Righter, Eds. (University of Arizona Press, 2000), pp. 323–338.
18. P. Papale, Modeling of the solubility of a one-component H_2O or CO_2 fluid in silicate liquids. *Contrib. Mineral. Petrol.* **126**, 237–251 (1997).
19. Z. Zhang *et al*., Primordial metallic melt in the deep mantle. *Geophys. Res. Lett.* **43**, 3693–3699 (2016).
20. R. M. Canup, Dynamics of lunar formation. *Annu. Rev. Astron. Astrophys* **42**, 441–475 (2004).
21. Y. Miyazaki, J. Korenaga, On the timescale of magma ocean solidification and its chemical consequences: 2. compositional differentiation under crystal accumulation and matrix compaction. *J. Geophys. Res.: Solid Earth* **124**, 3399–3419 (2019).
22. G. F. Davies, Stirring geochemistry in mantle convection models with stiff plates and slabs. *Geochim. Cosmochim. Acta* **66**, 3125–3142 (2002).
23. D. Porcelli, A. Halliday, The core as a possible source of mantle helium. *Earth Planet. Sci. Lett.* **192**, 45–56 (2001).
24. M. A. Bouhifd, A. P. Jephcoat, V. S. Heber, S. P. Kelley, Helium in Earth's early core. *Nat. Geosci.* **6**, 982–986 (2013).
25. P. L. Olson, Z. D. Sharp, Primordial helium-3 exchange between Earth's core and mantle. *Geochem. Geophys. Geosyst.* **23**, e2021GC009985 (2022).
26. S. Mukhopadhyay, R. Parai, Noble gases: A record of Earth's evolution and mantle dynamics. *Annu. Rev. Earth Planet. Sci.* **47**, 389–419 (2019).
27. Y. Li, L. Vočadlo, C. Ballentine, J. P. Brodholt, Primitive noble gases sampled from ocean island basalts cannot be from the Earth's core. *Nat. Commun.* **13**, 1–9 (2022).
28. A. S. Roth *et al*., The primordial He budget of the Earth set by percolative core formation in planetesimals. *Geochem. Perspect. Lett.* **9**, 26–31 (2019).
29. M. Landeau *et al*., Metal-silicate mixing by large Earth-forming impacts. *Earth Planet. Sci. Lett.* **564**, 116888 (2021).
30. R. Brooker *et al*., The 'zero charge' partitioning behaviour of noble gases during mantle melting. *Nature* **423**, 738–741 (2003).
31. V. S. Heber, R. A. Brooker, S. P. Kelley, B. J. Wood, Crystal-melt partitioning of noble gases (helium, neon, argon, krypton, and xenon) for olivine and clinopyroxene. *Geochim. Cosmochim. Acta* **71**, 1041–1061 (2007).
32. S. S. Shcheka, H. Keppler, The origin of the terrestrial noble-gas signature. *Nature* **490**, 531–534 (2012).
33. Si. Karato, Physical basis of trace element partitioning: A review. *Am. Mineral.* **101**, 2577–2593 (2016).
34. E. J. Garnero, A. K. McNamara, S. H. Shim, Continent-sized anomalous zones with low seismic velocity at the base of Earth's mantle. *Nat. Geosci.* **9**, 481–489 (2016).
35. J. C. Rosas, J. Korenaga, Rapid crustal growth and efficient crustal recycling in the early Earth: Implications for Hadean and Archean geodynamics. *Earth Planet. Sci. Lett.* **494**, 42–49 (2018).
36. V. Solomatov, R. El-Khozondar, V. Tikare, Grain size in the lower mantle: Constraints from numerical modeling of grain growth in two-phase systems. *Phys. Earth Planet. Inter.* **129**, 265–282 (2002).
37. P. Koelemeijer, A. Deuss, J. Ritsema, Density structure of Earth's lowermost mantle from Stoneley mode splitting observations. *Nat. Commun.* **8**, 15241 (2017).
38. M. S. Thorne, E. J. Garnero, S. P. Grand, Geographic correlation between hot spots and deep mantle lateral shear-wave velocity gradients. *Phys. Earth Planet. Inter.* **146**, 47–63 (2004).
39. J. R. Reimink *et al*., Tungsten isotope composition of Archean crustal reservoirs and implications for terrestrial μ^{182}W evolution. *Geochem. Geophys. Geosyst.* **21**, e2020GC009155 (2020).
40. J. Korenaga, Urey ratio and the structure and evolution of Earth's mantle. *Rev. Geophys.* **46**, RG2007 (2008).
41. D. Porcelli, T. Elliott, The evolution of He isotopes in the convecting mantle and the preservation of high ^{3}He/^{4}He ratios. *Earth Planet. Sci. Lett.* **269**, 175–185 (2008).
42. K. Burke, B. Steinberger, T. H. Torsvik, M. A. Smethurst, Plume generation zones at the margins of large low shear velocity provinces on the core-mantle boundary. *Earth Planet. Sci. Lett.* **265**, 49–60 (2008).
43. N. H. Sleep, Gradual entrainment of a chemical layer at the base of the mantle by overlying convection. *Geophys. J. Int.* **95**, 437–447 (1988).
44. S. Zhong, B. H. Hager, Entrainment of a dense layer by thermal plumes. *Geophys. J. Int.* **154**, 666–676 (2003).
45. M. Ishii, J. Tromp, Constraining large-scale mantle heterogeneity using mantle and inner-core sensitive normal modes. *Phys. Earth Planet. Inter.* **146**, 113–124 (2004).
46. H. C. Lau *et al*., Tidal tomography constrains Earth's deep-mantle buoyancy. *Nature* **551**, 321–326 (2017).
47. A. K. McNamara, A review of large low shear velocity provinces and ultra low velocity zones. *Tectonophysics* **760**, 199–220 (2019).
48. S. Labrosse, J. Hernlund, N. Coltice, A crystallizing dense magma ocean at the base of the Earth's mantle. *Nature* **450**, 866–869 (2007).
49. N. Coltice, M. Moreira, J. Hernlund, S. Labrosse, Crystallization of a basal magma ocean recorded by helium and neon. *Earth Planet. Sci. Lett.* **308**, 193–199 (2011).
50. A. W. Hofmann, W. M. White, Mantle plumes from ancient oceanic crust. *Earth Planet. Sci. Lett.* **57**, 421–436 (1982).
51. U. R. Christensen, A. W. Hofmann, Segregation of subducted oceanic crust in the convecting mantle. *J. Geophys. Res.* **99**, 19867–19884 (1994).
52. E. Mulyukova, B. Steinberger, M. Dabrowski, S. V. Sobolev, Survival of LLSVPs for billions of years in a vigorously convecting mantle: Replenishment and destruction of chemical anomaly. *J. Geophys. Res.: Solid Earth* **120**, 3824–3847 (2015).
53. V. Solomatov, C. Reese, Grain size variations in the Earth's mantle and the evolution of primordial chemical heterogeneities. *J. Geophys. Res.* **113**, B07408 (2008).
54. J. Korenaga, Thermal evolution with a hydrating mantle and the initiation of plate tectonics in the early Earth. *J. Geophys. Res.* **116**, B12403 (2011).